A novel approach for the realization of thin glass substrates for optical mirrors

Vecchi, G., Basso, S., Canestrari, R., Civitani, M., Ghigo, M., et al.

G. Vecchi, S. Basso, R. Canestrari, M. Civitani, M. Ghigo, J. Hołyszko, G. Pareschi, B. Salmaso, "A novel approach for the realization of thin glass substrates for optical mirrors ," Proc. SPIE 10706, Advances in Optical and Mechanical Technologies for Telescopes and Instrumentation III, 107060H (10 July 2018); doi: 10.1117/12.2313508

Event: SPIE Astronomical Telescopes + Instrumentation, 2018, Austin, Texas, United States

A novel approach for the realization of thin glass substrates for optical mirrors

G. Vecchi*, S. Basso, R. Canestrari, M. Civitani, M. Ghigo, J. Hołyszko[1], G. Pareschi, B. Salmaso
INAF-Brera Astronomical Observatory, Via E. Bianchi 46, 23807 Merate, Italy

ABSTRACT

We present a manufacturing process based on the deterministic polishing and figuring of thin glass substrates (shells), with thickness ranging from 0.5 up to a few millimeters, in "stand-alone" configuration or as part of a composite sandwich structure with low-density core. The methods will be well suited for a broad range of applications in astronomy like, e.g., the production of thin substrates for adaptive optics, the realization of sandwiched lightweight segments for the mirrors of future ground-based and space telescopes, and the realization of low-cost mirrors for amateur astronomy telescopes. The method foresees the pre-shaping of thin glass substrates via hot slumping technology followed by high-precision form correction of the optical surfaces via computer-controlled bonnet and ion beam figuring technologies. During the phase of bonnet polishing of a shell in stand-alone configuration, a removable holder stiffens it temporarily. This paper describes the main steps of the process under study and reports on the realization of the first prototypes.

Keywords: Substrates for adaptive optics, Substrates for active space optics, Lightweight astronomical mirrors, Sandwich mirrors, Thin glass shells, Glass slumping, Sub-aperture polishing

1. INTRODUCTION

The production on large scale of thin shell and lightweight mirrors represents an important objective for the implementation of future astronomical ground-based and space telescopes. For instance, adaptive optics are crucial components in present and future optical ground-based telescopes, as they compensate for the atmospheric turbulence by changing their shape at high frequency rate [1]. Thin glass shells are key elements for adaptive optics technology [2, 3]. The shell has an aspheric profile with a typical surface Root Mean Square (RMS) error of few tens of nanometers within 100 mm scale. In addition, future space telescopes will require larger apertures while complying with launch limitations on the mass. Thin glass shells, coupled with lightweight supporting structures [4-6], identify as key units for the development of active optics for future space telescopes, as they reduce the mass, while keeping the necessary stiffness. Methods for manufacturing such thin and flexible optics were developed, and allowed to reach the ultimate performance required by modern large telescope infrastructures. The manufacturing process used up to now relies on the thinning and grinding of high quality thick blanks in combination with stress polishing [2], stressed lap figuring [7], polishing and figuring [3, 8] technologies. It is clear that the thinning procedure, which is the common baseline to all these different approaches, is adequate for the production of single pieces, but it is not well suited for the production of large number of segments required for the assembly of large segmented adaptive or active systems.

In this paper, we present a different and innovative concept to manufacture thin glass substrates or shells. In this approach, the process starts procuring flat sheets of high-quality glass commercially available off-the-shelf. They have the desired thickness in the 1-2 mm range, tight specifications on the thickness uniformity and low micro-roughness. In its first phase, our concept provides the pre-shaping of the glass foils by hot slumping technology, which is based on the replication of the surface of a master mold. In the second phase of the process, which is the focus of the present work, the shape error remaining on the surface after slumping is addressed by high-precision sub-aperture polishing and figuring technologies directly applied on the thin glass shells. This method may represent an attractive approach to reduce time and cost by avoiding the step of thinning and grinding of high quality blanks. The hot slumping is based on the replica concept which is another cost saving asset, particularly in the framework of the production of series of identical or similar optics, as for large segmented primary mirrors. In Section 2, we describe the metrology and the first test of bonnet polishing applied to a thin slumped shell, reporting on the results obtained.

*gabriele.vecchi@brera.inaf.it; phone +39 02 72320478; fax +39-02 72320601; www.brera.inaf.it
[1]now at Officina Stellare s.r.l.

Advances in Optical and Mechanical Technologies for Telescopes and Instrumentation III, edited by
Ramón Navarro, Roland Geyl, Proc. of SPIE Vol. 10706, 107060H · © 2018 SPIE
CCC code: 0277-786X/18/$18 · doi: 10.1117/12.2313508

In Section 3, we introduce a further option in our fabricating concept, the lightweight sandwich mirror. This type of structure represents a technological driver for the development of future ground and space telescopes [9-11]. After the slumping phase, the glass shell is stiffened by assembling it into a sandwich mirror, with the purpose to freeze the floppy shape of the shell into a rigid but lightweight structure [12]. Afterwards, sub-aperture figuring technologies can take the process over [13]. We report on the first results obtained by applying the bonnet polishing technology on a lightweight sandwich mirror prototype.

1.1 Hot slumping technology

The development of the technology of hot slumping of glass started at INAF-Brera Astronomical Observatory in the past decade, in the framework of E-ELT Design Study financed by the European Community under OPTICON-FP6 [12, 14].The aim was to enable the production of a large number of thin glass segments for adaptive optics. The process occurs into an oven, where a flat, thin foil of glass is placed on top of a master mold. The surface of the mold is previously figured to meet the (complementary) target shape with high accuracy. After applying a suitable thermal cycle, the heated glass softens enough to slump onto the mold surface, copying its shape. After cooling down the system to room temperature, the slumped glass shell is released from the mold and ready for the deposition of any reflective coating. The results achieved with hot slumping were encouraging but still with an error too high compared to the requirements (surface RMS error achieved >100 nm versus a requirement <20 nm over 100 mm spatial scale). In the present study, we consider shells made in BOROFLOAT® 33 glass, 130 mm wide and 2 mm thick. They were slumped to a spherical shape in the early stage of the development of the hot slumping process at INAF-Brera Astronomical Observatory, together with larger shells up to 500 mm [15], which will be considered for future activity.

1.2 Deterministic polishing and figuring technology

In the proposed concept, we plan to carry out the post-slumping correction of the optical surface via deterministic sub-aperture figuring/polishing technologies. In this study, we consider the bonnet polishing technology, while we aim to apply Ion Beam Figuring (IBF) in the next activity.

At INAF-Brera Astronomical Observatory, the 1200 model of the IRP (Intelligent Robotic Polisher) series machine made by Zeeko Ltd. in UK is used [16, 17]. The typical correction process relies on a sub-aperture tool, namely, the bonnet, that polishes the surface and corrects its form while is scanning through the workpiece by following a defined path. The bonnet-polishing tool is inflated by air pressure and is usually applied covered with a polishing medium such as polyurethane foam. The robotic arm of the machine is equipped with nozzles delivering a temperature-controlled and density-monitored abrasive slurry. The bonnet is pressed against the surface by an offset of a few hundreds of microns, realizing the tool-workpiece contact spot. The material removal rate is proportional to the relative surface speed and to the pressure applied to the workpiece, according to the Preston model. Since surface speed and pressure are usually set constant into a run, the local removal is proportional to the dwell time of the tool at any position. For a given set of machine and process parameters, a dwell time matrix is calculated according to the removal required to correct the measured error map of the surface. Finally, the machine executes the dwell time matrix by varying the tool speed along the predefined path. Tools of different size address different intervals of the spatial frequency error range. Customized rigid tools can smooth out the spatial frequencies not correctable by the bonnet.

IBF technology [18] is well suited for the correction of low frequency errors on the thin slumped shells when the range of the residual error is of few hundreds of nanometers Peak-to-Valley (PV). The IBF technology employs a sub-aperture beam of accelerated ions to remove material from an optical surface. The dwell time principle to correct the shape errors applies similarly to the bonnet technology, while the contactless characteristic of the ion beam is greatly advantageous when it is required to correct the shape of near-edge zones, as for segmented mirrors [19].

2. THIN GLASS SHELLS

2.1 Metrology of thin glass shells

Generally, in order to manufacture optics compliant to tight requirement on surface form error, it is mandatory to have a corresponding metrological capability of the optical surfaces. In particular, this task is a non-trivial one when it comes to measure the surface shape of thin optics like the shells of glass investigated here, as they tend to sag due to gravity, and to deform depending on the supporting mount. Before performing the interferometric measurements to evaluate the surface form error of thin glass shells, we performed Finite Element Method (FEM) simulation to set the test shell into a configuration that minimizes the deformation induced on the optical surface.

The mounting system used for the interferometric measurements is a classic 2-points support in the lower part with a vertical resulting component almost equal to the mass of the glass substrate and a third point on the top that acts like a stopper to prevent the glass sample from falling backwards. In this upper point, the reaction force is very low and essentially along the horizontal direction. The support was analysed with FEM simulation, optimizing two parameters: the distance between the two points in the lower side and the distance of the upper point from a vertical plane passing through the two lower points. If we support the glass substrate in a nominal vertical position, a PV of 67 nm characterizes the gravity deformation on the optical surface. In order to reduce this deformation we moved the upper point backwards to tilt the glass substrate. We can decrease the total PV to less than 20 nm if the upper point is retreated of 1.5±0.3 mm, like shown in Fig.1. The distance between the two lower points is a less critical parameter and this length is 68 mm.

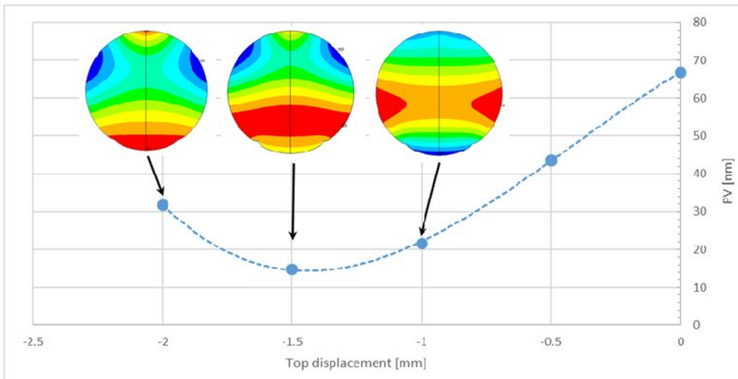

Figure 1. Optimization of the glass sample orientation as respect to the verticality. The lowest deformation occurs when the upper point is retreated of 1.5 mm from the vertical position.

We used a Zygo GPI series Fizeau interferometer equipped with a 4-inch f/3.3 transmission sphere to measure the form error map of the thin shells. These shells of BOROFLOAT® 33 glass were made from circular disks of 130 mm diameter and 2 mm thickness, and they were slumped to a spherical shape with radius of curvature of about 4 m. The back surface of the shell was rough not to disturb the measurements of the front surface. We set a relay mirror to fold the interferometric setup and fit within the optical bench. In this study, we employed an available non-kinematic mount to support the thin shell sample, as shown in Fig.2A. We modified this supporting mount according to the results of FEM analysis, therefore, to let the glass sample lean backwards by about 1.5 mm and sustained on three-points. Our repeatability error was still too high to appreciate the change of gravity deformation with the sample orientation, as predicted by FEM and shown in Fig.1. Nevertheless, the application of the FEM prescription allowed us to improve the repeatability of the alignment by eliminating the variable astigmatic deformation, which commonly appears when clamping the sample on its top edge. We performed a repeatability test by pick the sample up and put it back down on the mount and comparing the repeated measurements. Fig.2B shows the error map of about 12 nm RMS, obtained after subtraction of two repeated measurements. Such changes of shape on the optical surface could be traced back to the non-kinematic V-shaped mount, as a different stress was exerted on the flexible shell at each repositioning.

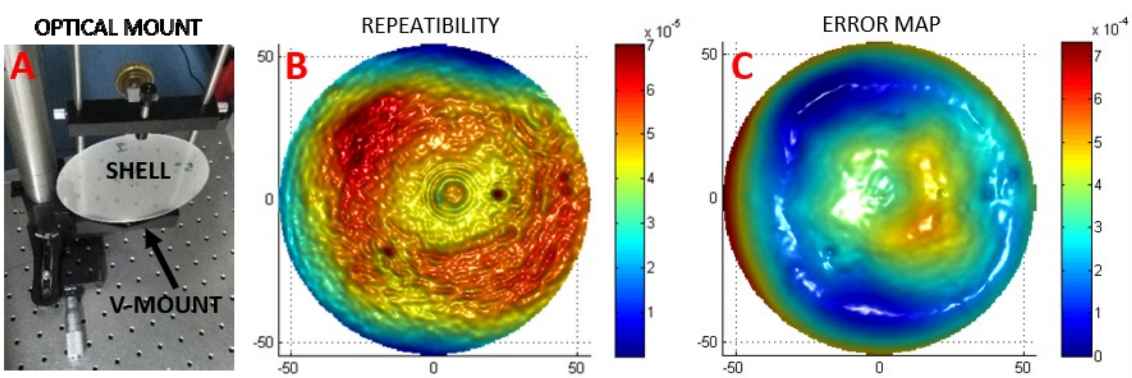

Figure 2. A. The 2 mm thick slumped shell supported on a three-point non-kinematic mount. B. Repeatability error map, 12 nm RMS. C. Error map of the slumped shell over 110 mm clear aperture, 128 nm RMS after removal of tilt and power terms. Color scales are in millimeters.

Fig.2C shows the measured residual error map of the thin slumped shell after removal of tilt and power terms. Both maps refer to a clear aperture set to 110 mm, the aperture of reference throughout this study. The “free-standing” error map shown in Fig.2C has an RMS value of 128 nm, and PV of 736 nm. It does represent here the input data feeding the bonnet polishing process.

2.2 Temporary stiffening of the thin glass shell

The thin substrates of glass need to be stiffened temporarily by a removable holder during the phase of bonnet polishing. This is required as the pressure applied in the contact spot on the optical surface would deform it locally, or even break it, leading the dwell-time-based material removal process to inconsistent results. We designed the stiffening holder to become the mechanical interface to the polishing machine but also to the interferometric setup. In fact, we aimed to check the evolution of the surface error throughout the iterative process of bonnet polishing, while keeping the slumped shell fixed on its stiffening holder. This procedure has the advantage to eliminate the need of releasing the glass shell from the holder after each polishing run in order to verify the status of the surface error. To this purpose, the ideal condition happens when the stiffening procedure does not modify the shape of the optical surface measured in the “free-standing” configuration. Otherwise, when the stiffening does deform the optical surface: 1) some residual error due to print-through effect is expectable during the polishing phase; 2) the measure of the “free-standing” shape is indirect and less accurate. We made the holding flange in Inox AISI 304, and we machined its top surface to meet the nominal radius of curvature of 4 m, therefore, matching the curvature of the slumped shell. Fig.3A shows the glass shell fixed on the holder by a blocking wax characterized by a melting point near 40°C. Fig.3B shows the shape error map of the holder surface as respect to the target spherical shape. This map is the interpolation of a grid of discrete points measured with a Coordinate Measuring Machine (CMM), whose accuracy is of the order of few microns. Actually, the turning process introduced a significant shape error, in particular, a prominent bulge featuring in the center of the holder surface, exceeding the nominal sphere by about 50 µm.

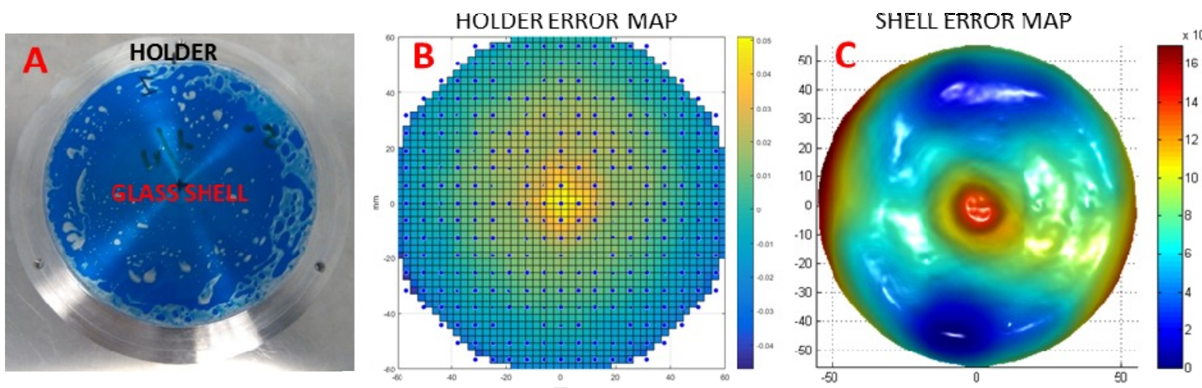

Figure 3. A. Slumped shell blocked onto a stainless steel holder using a (blue-colored) thermal wax. B. Interpolated error map of the holder with respect to the nominal sphere with 4 m radius of curvature. The range of the colored scale is 100 µm. C. Error map of the shell stiffened on the holder, over 110 mm clear aperture, after removal of tilt and power terms. Color scales are in millimeters.

Fig.3C shows the error map of the shell stiffened on the holder, measured with the interferometer over a 110 mm clear aperture, after removal of tilt and power terms. The shape of the optical surface appears deeply modified with respect to its “free-standing” shape, shown in Fig.2C. Both RMS and PV values increased by more than a factor two, featuring 296 nm and 1700 nm, respectively. It is likely that the mechanical mismatch between the Inox holder and the BOROFLOAT® 33 shell contributed to the measured deformation. We repeated measurements over a long (one-month) timeframe to assess the stability of the blocking wax, and we found the repeatability error was below 20 nm RMS, including the contribution due to mounting/unmounting the system in the interferometric setup. Corrective actions are planned to minimize any change of shape on the optical surface, by improving either the holder shape or the wax blocking process.

2.3 Bonnet polishing of the thin glass shell

We finally applied the bonnet polishing process to the thin shell blocked onto the holder. The sub-aperture polishing was set to address the low frequency content, with spatial wavelength >10-20 mm. Fig.4 shows the trend of the error map through the first two corrective runs. The 128 nm RMS value of the initial "free-standing" error map dropped to 31 nm RMS expected value after run2. We derived the error maps after run1 and run2 shown in Fig.4 (center and right panels) from the interferometric measurements on the blocked shell. Each of these two maps, with its RMS value, is the "free-standing" residual error map foreseen after each run of polishing. We inferred it by subtracting the removal of material measured at each run from the initial error map (left panel in Fig.4). This method becomes progressively less accurate as larger deformation is induced on the surface, and as the amplitude of the targeted error of the polishing process gets comparatively smaller.

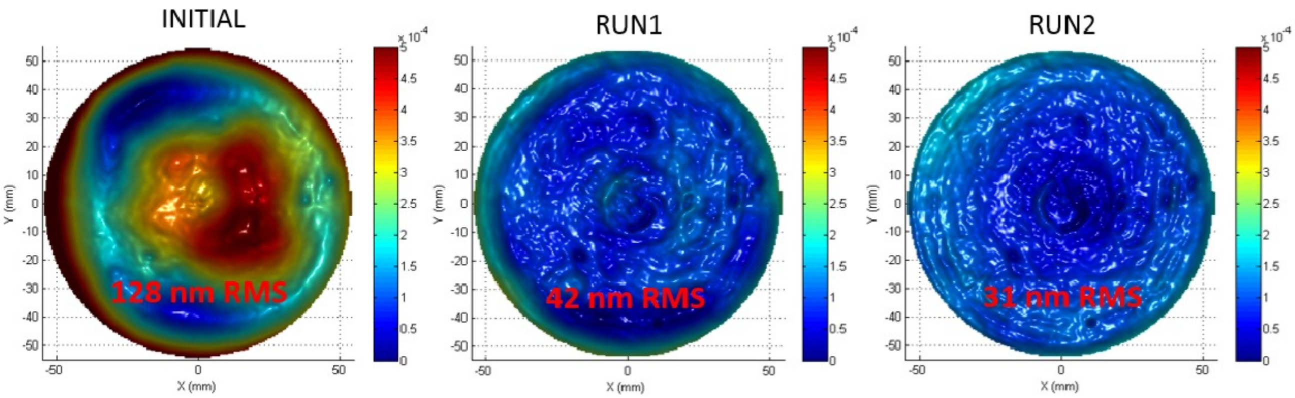

Figure 4. Error map trend as deduced from the shape measured on the blocked shell. Tilt and power terms were removed. The RMS values are reported. Left map is the same as in Fig.2C. Amplitude range is limited to 500 nm (color scales in millimeters) for a better view of the central and right maps.

We also tested a third run of polishing (not shown) which apparently improved a little further the figures, providing 29 nm RMS (instead of 31 nm) and 190 nm PV over the 110 mm aperture. We found that our sensitivity to appreciate any further small improvement in the surface accuracy was limited because 1) we were estimating small residual errors by subtraction between large error maps, and 2) we were approaching the repeatability error of our measuring setup. Therefore, we stopped the iteration with bonnet polishing, we released the glass shell from the holder and we measured it again in the real "free-standing" configuration as shown in Fig.2A. Fig.5 shows the surface error map of the thin slumped shell, with 38 nm RMS and 206 nm PV over 110 mm aperture and after removal of tilt and power terms.

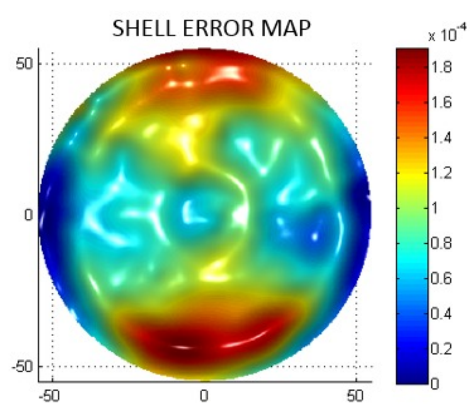

Figure 5. Residual error map after the bonnet polishing correction, and after releasing the shell from the stainless steel stiffening support. Tilt and power terms were removed. RMS and PV values are 38 nm and 206 nm, respectively. Color scales in millimeters.

The bonnet polishing improved the surface accuracy of the slumped shell by a factor three (from 128 nm down to 38 nm RMS) in about two hours of processing time. The remaining error visible in Fig.5 is largely associated to an astigmatism component, unexpected during the polishing process as depicted in Fig.4. We noticed some similarity existing between the pattern of this error map and the error map (with reverse sign) measured on the blocked shell, shown in Fig.3C. As a hypothesis, the astigmatism might partly relate to the mentioned print-through effect due to the strong deformation induced on the optical surface while blocked onto the rigid holder. Further investigation is required to understand the origin of this finding. It is worth to notice that after removal of the astigmatism term, the residual error is halved, reaching 19 nm RMS and 151 nm ($\lambda/4$) PV over 110 mm aperture, close to the repeatability error of the measuring system employed in this study.

3. LIGHTWEIGHT SANDWICHED GLASS MIRRORS

Lightweight yet rigid sandwiched glass mirrors may find relevant applications in segmented ground and space telescopes. At INAF-Brera Astronomical Observatory, we investigated the feasibility of assembling thin shells of slumped glass into stiff but lightweight composite structures since the past decade. A detailed description of this earlier work is reported in Ref. [12]. A lightweight (areal density ~16 Kg/m^2) sandwiched mirror prototype was manufactured, characterized and Aluminum coated. Fig.6A shows the layout conceived to freeze the flexible, slumped glass substrate into a rigid sandwiched mirror. The sandwich structure was stacked directly on top of the slumping mold, and it included: 1) the slumped BOROFLOAT® 33 glass shell, 130 mm wide, 2 mm thick and with 4 m radius of curvature; 2) a pre-shaped glass foam substrate and 3) a flat BOROFLOAT® 33 glass on the backside with size and thickness equal to the front shell. The foam substrate provided the stiffness to the final mirror while keeping it lightweight, while the symmetric sandwich-like structure guaranteed the structural stability. The glue used to make the sandwich was a low percentage shrinkage epoxy. Fig. 6B displays the mirror prototype after the Al-coating of the optical surface.

Figure 6. A. Layout of the permanent stiffening phase. B. The sandwiched glass mirror prototype after the aluminization of the optical surface. C. The same prototype after removal of the Al coating, held by an Inox flange designed as an interface to the metrology and polishing stations.

In the study in Ref. [12], we also observed that the shape of the slumped shell did not change significantly after the stiffening/ assembling into the sandwiched structure. Recently, we decided 1) to check the status of this old prototype mirror, and 2) to improve its shape accuracy by applying a sub-aperture figuring process, like the bonnet polishing in this study. This is a convenient approach to correct the residual surface error of the thin slumped shells after their permanent stiffening into the sandwiched structures. We removed the Al coating to perform new interferometric measurements of the (slumped) spherical side of the sandwich mirror. This measurement campaign provided the surface error map to begin the bonnet polishing corrective process. Meanwhile, it provided the opportunity to evaluate the structural stability of this prototype over a temporal span of about ten years. Fig.7 shows two error maps of the optical surface of the same prototype mirror. The left panel shows the error map measured in the context of Ref. [12], whereas the right panel shows the map measured recently, after the stripping of the Al-coating. The measurements were performed using two setups with different optical layouts. Tilt and power terms were removed, and the measured aperture was kept to 110 mm in both cases. We found impossible to achieve a full quantitative comparison, as the two series of measurements followed different prescriptions. However, they look rather similar, the main common features are a few digs or pronounced minima most probably caused by dust particles trapped at the mold-glass interface during the hot slumping process. RMS and PV figures match well in the new and old error maps, and are close to 327 nm (~$\lambda/2$) and 2600 - 2800 nm (~4.2λ), respectively.

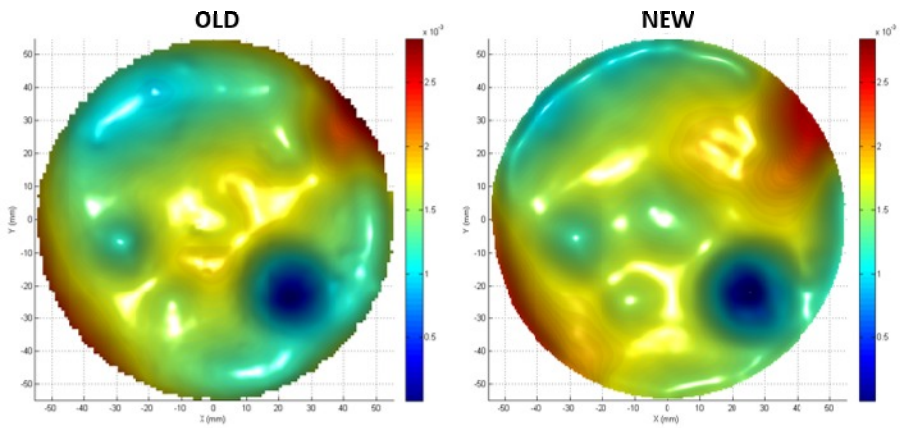

Figure 7. Error map of the optical surface of the prototype mirror. Left: measurement performed within the study in Ref. [12]. Right: Recent measurement after coating removal, with different support and interferometric setup. Tilt and power terms were removed. RMS and PV values are very similar for both maps, ~λ/2 and ~4.2λ respectively. The color scales are in millimeters.

3.1 Bonnet polishing of the sandwiched glass mirror

We applied the bonnet polishing process to the sandwiched glass mirror surface targeting the low frequency content, with spatial wavelength >10 mm. Fig.8 shows the trend of the error map as measured with the interferometric setup after each run of polishing. The RMS values decreased by an order of magnitude, from 328 nm (~λ/2 RMS) to 27 nm (~λ/23 RMS), over the 110 mm measured aperture. It is worth to remark that the deepest feature on the optical surface was associated to the presence of dust during the hot slumping process. This feature is the main source for the large PV in the initial error map, therefore, for the large removal of material required in the phase of bonnet polishing. A tighter requirement of cleanliness during the slumping phase would already be effective in reducing the overall processing time.

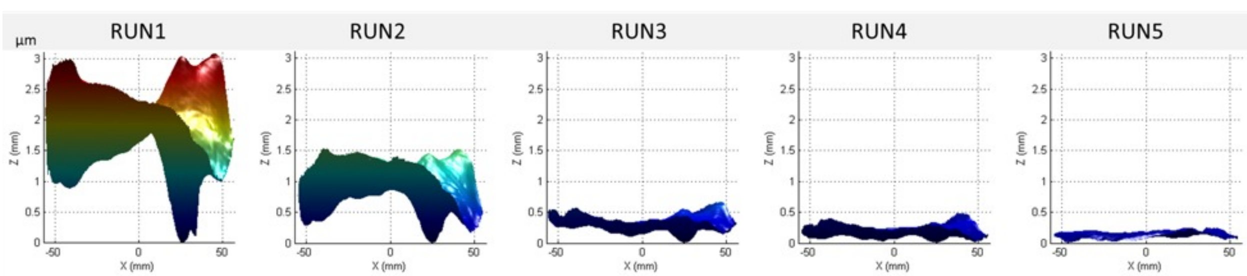

Figure 8. Trend of the surface error map through the iterative bonnet polishing on the sandwiched glass mirror. Tilt and power terms were removed. The RMS values decreased from 328 nm (~λ/2 RMS) to 27 nm (~λ/23 RMS) over the 110 mm measured aperture (color scale in microns).

Fig.9 shows the residual error map measured over 100 mm aperture at the end of the bonnet polishing iteration. After removal of tilt and power the RMS and PV were reduced to 22 nm and 134 nm (~λ/29 and ~λ/4.7) values, respectively. We obtained this encouraging result by targeting the correction of error with wavelength larger than 10 mm. On the other hand, Fig.9 shows the presence of a pattern constituted of straight and orthogonal features crossing the error map. We attributed the origin of these features to some perturbation/fluctuation of process parameters occurring during the bonnet polishing. Probably, small density variations of the circulating abrasive fluid caused small changes in the removal rate while the tool was following a raster path. This explains the pattern of straight features, while their orthogonal crossing is due to the change of raster orientation by 90 degrees over successive runs.

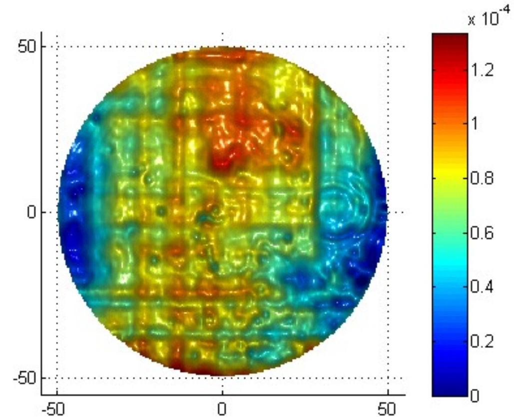

Figure 9. Surface error map after bonnet polishing on the sandwiched glass mirror. Tilt and power terms were removed. The RMS and PV over 100 mm measured aperture reached 22 nm (~λ/29) and 134 nm (~λ/4.7), respectively. The color scale is in millimeters.

These error features have wavelength close or shorter than the smallest size of the bonnet contact spot on the surface. The deterministic removal of this mid spatial frequency pattern is very difficult/inefficient to accomplish with a sub-aperture tool scanning through the surface with the dwell-time principle. Mid-high spatial frequencies removal is achievable by specific tools more rigid than the bonnet.

4. CONCLUSIONS

In this paper, we presented and discussed a method for manufacturing high-precision thin and lightweight glass shell mirrors. Thin glass shells are key elements driving the development of both adaptive optics solutions in ground-based telescopes and of active optics designs for future large space telescopes. Another innovative concept under development also relies on thin glass shells to make sandwiched mirrors of high structural stability, for lightweight-segmented mirrors of future ground-based and space telescopes. We aim to demonstrate that the presented manufacturing approaches are feasible and advantageous, as they leverage on cost-effective solutions for glass procurement, mirror segments replication and contactless ion figuring. The presented fabricating concept takes advantage of the commercial off-the-shelf availability of high-quality large sheets of glass, which have tight thickness control and low micro-roughness. Then, a highly accurate replication mold is used to thermally-shape the thin glass substrates by slumping technology. The following sub-aperture polishing and ion beam figuring processes apply directly on the thin slumped shells to correct the residual surface errors.

The preliminary results reported on 2 mm thick and ~100 mm size glass substrates are encouraging, and focus on the verification that bonnet-polishing technology does improve the shape accuracy of thin slumped optics. During bonnet polishing a force is applied on the shell surface, therefore, the shell needs to be blocked temporarily on a rigid support. The shape accuracy improved after bonnet polishing from ~λ/5 RMS to ~λ/17 RMS over 110 mm aperture. We also tested the bonnet polishing onto a sandwich glass mirror with a small areal density of ~16 Kg/m^2. The front optical surface of this prototype was made by a slumped thin shell, where we reported an improvement of the surface accuracy by an order of magnitude, from ~λ/2 RMS down to ~λ/23 RMS over 110 mm.

Next activities will be devoted to improve the stiffening phase of the shell by reducing the induced deformation on it. This will help to assess the evidence of any associated print-through error, minimize it, and improve the bonnet polishing performance. We aim also to: 1) test the IBF process on the thin slumped shell after bonnet polishing; 2) improve the interferometric setup to reduce the repeatability error of the measurements, and 3) test and adopt solutions to mitigate/eliminate the mid spatial frequencies. In this first study, the size of the optics was limited to 130 mm (110 mm aperture considered). On a longer timescale, our purpose is to demonstrate the feasibility of the manufacturing process by upgrading to a 500 mm size scale both the thin slumped shell and the sandwich mirror configurations.

REFERENCES

[1] Madec, P. -Y., "Overview of deformable mirror technologies for adaptive optics and astronomy", Proc. SPIE 8447, 844705 (2012).

[2] Hugot, E., Ferrari, M., Riccardi, A., Xompero, M., Lemaître, G. R., Arsenault, R. and Hubin, N., "Stress polishing of thin shells for adaptive secondary mirrors", A&A 527, A4 (2011).

[3] Poutriquet, F., Rinchet, A., Carel, J. -L., Leplan, H., Ruch, E., Geyl, R. and Marque, G., "Manufacturing of glassy thin shell for adaptive optics: results achieved", Proc. SPIE 8447, 84472H (2012).

[4] Briguglio, R., Biasi, R., Gallieni, D., Vettore, C., d'Amato, F., Xompero, M., et al., "Laboratory demonstration of a primary active mirror for space with the LATT: large aperture telescope technology", Proc. SPIE 9904, 99046C (2016).

[5] Hallibert, P. and Zuccaro Marchi, A., "Developments in active optics for space instruments: an ESA perspective", Proc. SPIE 9912, 99121H (2016).

[6] Baiocchi, D., Burge J. H. and Cuerden, B., "Demonstration of a 0.5-m ultralightweight mirror for use at geosynchronous orbit", Proc. SPIE 4451, 86-95 (2001).

[7] Martin, H. M., Burge, J. H., Del Vecchio, C., Dettmann, L. R., Miller, S. M., Smith, B. and Wildi, F., "Optical fabrication of the MMT adaptive secondary mirror", Proc. SPIE 4007, 502-507 (2000).

[8] Briguglio, R., Xompero, M., Riccardi, A., Lisi, F., et al., "Development of Large Aperture Telescope Technology (LATT): test results on a demostrator bread-board", Proc. SPIE 10563, 105634F (2014).

[9] Burge, J., Cuerden, B., Miller, S., Crawford, B., Dorth, H., Sandler, D. and Wortley, R., "Manufacture of a 2-m mirror with glass membrane facesheet and active rigid support", Proc. SPIE 3782, 123-133 (1999).

[10] Catanzaro, B., Keane, D., Connell, S., Baiocchi, D., Burge, J., Maji, A. and Powers, M., "UItraLITE Glass/Composite Hybrid Mirror", Proc. SPIE 4013, 663-671 (2000).

[11] Devilliers, C., Du Jeu, C., Costes, V., Suau, A., Girault, N. and Cornillon, L., "New design and new challenge for space large ultralightweight and stable Zerodur® mirror for future high resolution observation instruments", Proc. SPIE 10563 105631I (2014).

[12] Canestrari, R., Ghigo, M., Pareschi, G., Basso, S. and Proserpio, L., "Investigation of a novel slumping technique for the manufacturing of stiff and lightweight optical mirrors", Proc. SPIE 7018, 70180D (2008).

[13] Shorey, A., Kordonski, W. and Tricard, M., "Magnetorheological finishing of large and lightweight optics", Proc. SPIE 5533, 99-107 (2004).

[14] Ghigo, M., Basso, S., Citterio, O., Mazzoleni, F., Vernani, D., "Manufacturing of lightweight glass segments for adaptive optics", Proc. SPIE 6272, 62720X (2006).

[15] Ghigo, M., Basso, S., Canestrari, R. and Proserpio, L., "Development of hot slumping technique and last optical performances obtained on a 500 mm diameter slumped segment prototype for adaptive optics", Proc. SPIE 7439 74390M (2009).

[16] Walker, D. D., Brooks, D., King, A., Freeman, R., Morton, R., McCavana, G. and Kim, S. -W., "The ‘Precessions’ tooling for polishing and figuring flat, spherical and aspheric surfaces", Opt. Express 11, 958-964 (2003).

[17] Vecchi, G., Basso, S., Civitani, M., Ghigo, M., Pareschi, G., Riva, M. and Zerbi, F. M., "A bonnet and fluid jet polishing facility for optics fabrication related to the E-ELT", Mem. S.A.It. 86, 408 (2015).

[18] Ghigo, M., Vecchi, G., Basso, S., Citterio, O., Civitani, M., Mattaini, E., Pareschi, G. and Sironi G., "Ion figuring of large prototype mirror segments for the E-ELT", Proc. SPIE 9151, 91510Q (2014).

[19] Civitani, M., Ghigo, M., Hołyszko, J., Vecchi, G. and Basso, S., "Ion beam figuring of thin glass plates: achievements and perspectives", Proc. SPIE 9905, 990578 (2016).